THE NATURE OF INTERLAYERING IN MIXED-LAYER ILLITE–MONTMORILLONITES

ROBERT C. REYNOLDS, JR.
U.S. Army Cold Regions Research and Engineering Laboratory and Earth Sciences Department,
Dartmouth College, Hanover, New Hampshire 03755

and

JOHN HOWER
Geology Department, Case Western Reserve University, Cleveland, Ohio 44106

Abstract – The nature of interstratification in mixed-layer illite–montmorillonites has been investigated by comparison of diffraction patterns of ethylene glycol and ethylene glycol monoethyl ether treated samples with calculated one-dimensional diffraction profiles. The calculated profiles take into account the effects of particle size distribution, chemical composition, and convolution factors as well as proportions of layers and interstratification type. On the basis of detailed matching of diffraction patterns of monomineralic illite–montmorillonites of known chemical composition it is concluded that there are three types of interstratification: (1) random, (2) allevardite-like ordering, and (3) super-lattice units consisting of three illite and one montmorillonite layers (IMII). By comparison of suites of calculated profiles with the diffraction patterns of many samples of illite–montmorillonites it is concluded that virtually all illite–montmorillonites with expandabilities from about 40 to 100 per cent are randomly interstratified (allevardite being exceptional); at <40 per cent montmorillonite layers they almost always have ordered interstratification. Allevardite-like ordering predominates in illite–montmorillonites which have ordered interstratification, with the IMII superlattice varieties confined to samples with about 10 per cent montmorillonite layers.

INTRODUCTION

THE EXISTENCE of mixed-layer clays has been known for several decades (Hendricks and Teller, 1942) and the abundance and petrological importance became obvious with the extensive work of Weaver (1956). Any investigation of mixed-layer clays – whether petrological or mineralogical in nature – hinges on the ability to interpret X-ray diffraction patterns of these structures. This ability is limited in part by such practical considerations as the complexity of many clay mineral assemblages, but more fundamentally by a lack of knowledge by most investigators of the effects of such factors as manner of interlayering and particle size distribution on the X-ray diffraction patterns.

Ordering involving a perfectly alternating sequence of two different layer types such as corrensite (Lippman, 1954) and allevardite (Brindley, 1956) can be recognized by an integral multiple series of (00*l*) reflections based on a large unit cell. These minerals, however, have a relatively limited distribution. By contrast, non-random interstratification involving a proportion of two types of layers different from 1:1 is less easily

recognized, because it gives rise to a sequence of (00*l*) reflections that is non-integral and is often mistakenly assumed to be random. This type of ordering has also been recognized, but has usually been reported as a unique occurrence (Byström, 1954; Sato, 1965) or without extension of the results to generalities (Hamilton, 1968; Maiklem and Campbell, 1965). Virtually every investigator has interpreted his diffraction patterns assuming random interstratification of the layers involved (e.g., Hower and Mowatt, 1966; Weaver, 1956; Burst, 1969).

From a petrological standpoint, the most interesting mixed-layer clays are undoubtedly illite–montmorillonites, for they are ubiquitous, are the best known chemically, and show a mineralogical variation that responds to pressure–temperature variations during diagenesis (Burst, 1969; Velde, 1969; Perry and Hower, 1969). A considerable body of literature exists – mainly by D. M. C. MacEwan and co-workers – treating the theoretical aspects of the diffraction effects of mixed-layer clays including illite–montmorillonite. In the writers' experience existing treatments are of limited use to the main body of

workers in the field of mixed-layer clays because: (1) the diffraction patterns are calculated assuming only random interstratification (MacEwan, Ruiz Amil, and Brown, 1961; Ross, 1968), or (2) the diffraction effects are presented only in terms of the mixing function with migration curves for the peaks (Ruiz Amil, García, and MacEwan, 1967). As will be shown, use of migration curves without comparison with a realistic calculated diffraction pattern can lead to serious errors of interpretation.

The object of this paper is to present the methods and results of one-dimensional diffraction profiles calculated by computer methods for examples of mixed-layer montmorillonite(glycol)–illite, and montmorillonite (ethylene glycol monoethyl ether)–illite. The calculations were performed by methods that are similar to those reported earlier (Reynolds, 1967), except that the original techniques for treating random interstratification were modified and extended to include conditions of nearest-neighbor and non-nearest-neighbor ordering. In addition, refinements were introduced into the calculated profiles to furnish a closer approach to real diffraction patterns. These refinements include: (1) a provision for a range of particle thicknesses rather than a single particle thickness, and (2) a controlled broadening function which is convolved upon the calculated pattern thereby simulating some of the effects of particle-size and instrumental broadening.

The Dartmouth General Electric time sharing computer system has made it possible to develop a rapid analog method for gaining information on clay structures. The ready availability of computer facilities, and the sophistication of the system, make it feasible for an investigator to use a reiterative system in which guesses are made concerning a clay structure, followed by a rapid evaluation of the consequences of such guesses. A numerical model of a clay structure can be rapidly modified to the point at which observed and calculated diffraction profiles are as similar as are two specimen runs from the same sample. At this point, it may be assumed that no more information can be extracted from the diffraction pattern, and that the structures are known as well as they can be, given the errors in the X-ray analytical system and the calculating technique.

Studies reported here demonstrate the power of this method and illustrate the types of ordering found in common occurrences of montmorillonite–illite. Samples are described in which (a) the interstratification is random, (b) the structure is allevardite-like (Brindley, 1956), involving an illite–montmorillonite superlattice (IM), randomly interstratified with additional illite, and (c) the structure consists of an IMII superlattice randomly

interstratified with illite. This latter condition appears to be common in potash bentonites, or indeed, in any glycolated montmorillonite–illite showing a strong diffraction maximum between 10·8 and 11·2 Å in addition to one at 9·6–10·0 Å. As confirmatory evidence, it is shown that similar agreement between observed and calculated patterns is obtained from the same clay parameters with the substitution of the interlamellar material ethylene glycol monoethyl ether into the clay by solvation, and into the simulated patterns by calculation. An appendix shows a series of calculated profiles for montmorillonite (glycol)–illite which demonstrates the effects of composition and ordering upon the diffraction profiles. The profiles in the appendix are readily applicable to the interpretation of X-ray diffraction patterns of mixed-layer illite–montmorillonites and cover the range of types known to the authors.

METHODS OF CALCULATION

Treatment of non-random interstratification

A modification of the MacEwan Fourier Transform Method that incorporates the effects of interlamellar scattering has been described earlier (Reynolds, 1967). This method was used as reported for cases of random interstratification, but was used in two modifications to provide for the simulation of ordered structures.

For conditions of nearest-neighbor ordering, and for cases of N (the number of silicate skeletons per crystallite) up to 13, matrices of frequency coefficients were computed by a newly developed program. All montmorillonite-illite arrays are generated for $N = 2$ to $N = 13$. These are sorted out so that for any N, three categories are summed separately, i.e., those with an illite on each end, those with a montmorillonite(glycol) on each end, and those with an illite on one end and a montmorillonite(glycol) on the other. The frequency of occurrence of each array in each set is computed by multiplying the frequency of the first interlamellar unit in a given array by the junction probabilities of all junctions in the array. The junction probabilities are defined, for the conditions of nearest-neighbor ordering, by (1) the proportion of illite or montmorillonite, and (2) one junction probability. The procedure is described by MacEwan (1958). Hence a typical matrix provides values for the summed frequencies of occurrence of all arrays that contain M montmorillonite units and 1 illite* units $[M + I \leq (N - 1)]$ with the

---

*A montmorillonite unit is defined as a glycol-filled interlamellar space, and an illite unit is a collapsed interlamellar space occupied by potassium.

added stipulation that the only terms included in a given summation are those with specified ends. The three matrices of frequency coefficients may be specified as $P^{I-I}_{(I,M)}$, $P^{M-M}_{(I,M)}$ and $P^{M-I}_{(I,M)}$. Each value in each of the three matrices is multiplied by $[N - (I+M)]$, where $I+M \leqq (N-1)$, in order to correct for end effects, and the final value gives the frequency of occurrence of a given spacing that is defined by the specified number of illite and montmorillonite units, viz, spacings with $I-I$ ends equal $[(I-1) . 10\,\text{Å}] + (M . 16\cdot9\,\text{Å})$, those with $M-M$ ends equal $(I . 10\,\text{Å}) + [(M-1) . 16\cdot9\,\text{Å}]$, and those with $I-M$ ends equal $[(I-\frac{1}{2}) . 10\,\text{Å}] + [(M-\frac{1}{2}) . 16\cdot9\,\text{Å})]$ (see Reynolds, 1967, p. 664–665). The remainder of the calculation proceeds as in the case of random interstratification.

A second modification of the random case computer program consists of the simple artifice of substituting the spacing of a superlattice unit into the calculation, together with its appropriate Fourier transform, in place of a single inter-lamellar position. Random statistics are used. Let P_ξ equal the proportion of superlattice units (IM) consisting of a potassium layer, a silicate skeleton, and a double glycol layer, and let P_ι equal the proportion of illite not involved in the superlattice. $P_\iota + P_\xi = 1$. A correction must be made to account for the fact that the hypothetical sample contains illite in two associations, in the superlattice, and as discrete layers. Hence, the proportion of illite in the sample, P_I, is not equal to P_ι. The following relationship holds, where P_M is the proportion of montmorillonite, and η is the number of silicate skeletons in the superlattice:

$$P_\xi = \frac{P_M}{1 - \eta . P_M}.$$

The proportion of illite, P_I, is simply equal to $1 - P_M$.

The frequency coefficients are computed according to the principles of random statistics, i.e., $P_\xi = P_{\iota,\xi} = P_{\xi,\xi}$ and $P_\iota = P_{\xi,\iota} = P_{\iota,\iota}$ (see MacEwan, 1961, p. 395). Note that $P_{\iota,\xi}$ does *not* mean the probability of occurrence of an $\iota\xi$ pair. Rather, it denotes the probability of a ξ *given* a ι. The probability of occurrence of an $\iota\xi$ pair, which may be written $P_{\iota\xi}$ is given by $P_\iota . P_{\iota,\xi}$.

The Fourier transform of the superlattice is calculated with respect to the center of the super-lattice. This position does not correspond to a center of symmetry on projection, therefore, the imaginary portion of the structure factor is not eliminated, and the Fourier transform of the super-lattice includes a sine summation as well as a cosine summation. The product of the complex structure factor and its complex conjugate is taken and this

is multiplied by the mixing function that applied to $\xi-\xi$ ends. For all other end pairs (see Reynolds, 1967, p. 665) that involve the superlattice, one end is centrosymmetric and its sine summation equals zero, thus eliminating the complex portion of the superlattice transform. For these cases, the relevant atomic factor is simply the product of the cosine summations of the two appropriate transforms.

This procedure is not rigorously correct. Individual hypothetical stacking arrays have different values of N, depending on the number of superlattice units involved. For example, in calculations of unordered structures, the number of silicate layers is one more than the number of interlamellar spaces. But in the case of the $IMII$ superlattice, each superlattice unit contains three silicate skeletons, thus in a given array $N = (3 \cdot \xi) + \iota + 1$, where ξ equals the number of superlattice units and ι equals the number of discrete illite units in a given array. The effective value of N for the calculation is larger than it would be for a condition of random interstratification of illite and montmorillonite interlamellar units and different arrays have different values of N even though $\xi + \iota$ is constant. The consequences of these theoretical limitations were evaluated as described below.

Calculations were compared, using this approach for allevardite-like ordering, with calculations made for the same structure but done "correctly", that is, by using non-random statistics. Differences between the two calculated patterns were minor, provided N was in the vicinity of 7 or above. The only detectable differences were (a) an increase in the amplitudes of background ripples, and (b) a decrease in the peak breadth, for patterns calculated by the superlattice modification. When a distribution of N values was used, the ripples were eliminated and the maxima were broadened somewhat. Only residual peak sharpness remained to distinguish the data computed using the super-lattice modification. The use of superlattice units, in conjunction with random statistics, represents a great saving in program complexity and computer time. In the case of complicated superlattice units (i.e., non-nearest-neighbor ordering), a "correct" solution, involving non-random statistics may present a problem of prohibitive mathematical complexity.

Particle size range

Calculations were made for a distribution of particle thickness by substituting for the last portion of the frequency coefficient $[N - (n_A + n_B)]$ (Reynolds, 1967, p. 664), the term

$$\Sigma_N q(N) . (N - Vn).$$

where $N > Vn$ (MacEwan, 1958, p. 66). N is the number of silicate layers, and $q(N)$ is the relative fraction of N layer crystallites in the hypothetical sample. Vn equals the number of interlamellar units of type A plus the number of units of type B. It is understood that for each term in the series, the number of interlamellar layers in the array (Vn) may not exceed a value that is one less than the number of silicate skeletons (N).

Line broadening

Calculated diffraction patterns were broadened by the application of the superposition theorem. There are many factors which contribute to peak breadth, arising from instrumental factors and the structural condition of the sample. An exact treatment would have involved a process of successive convolution that applied each of these functions sequentially. Instead, the final form of the breadth function was assumed to be gaussian, and this $(Y = e^{-k^2 e^2})$ function was applied to the calculated diffraction profiles. Breadth constants, k, were adjusted until a single value was found which gave good agreement between all calculated and all observed peak profiles for a given sample. The value for k was not varied with 2θ, even though particle size broadening is probably the most weighty portion of the broadening function
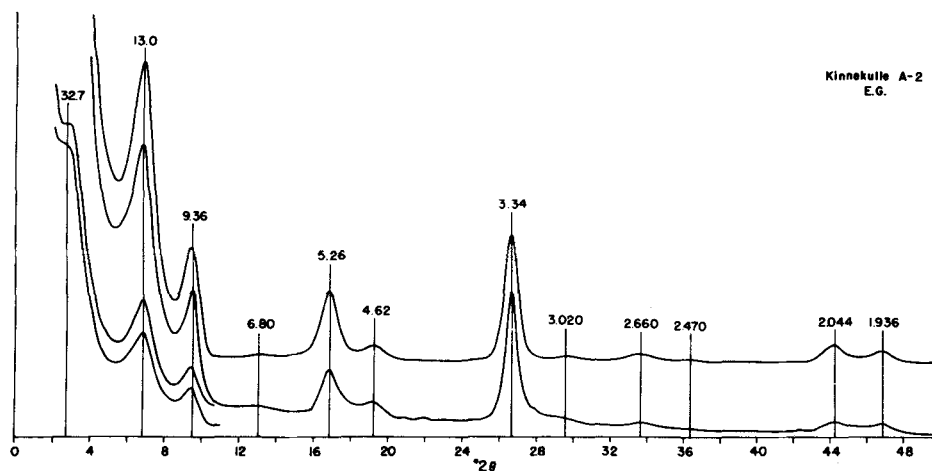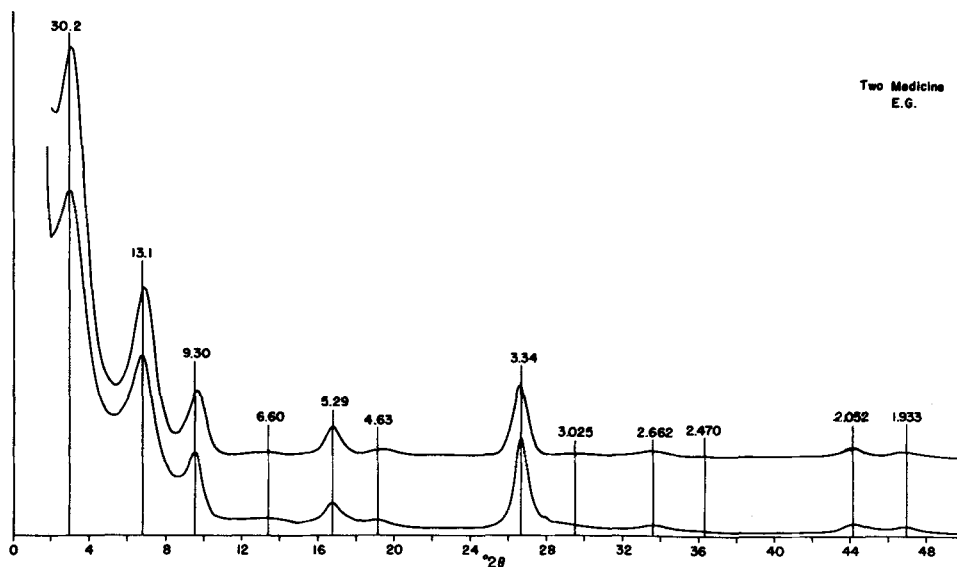

Fig. 1(a).

Fig. 1(b).

and is angle dependent. Over the small range of $0°$ to $25°\theta$, the change in the breadth constant is insignificant for work of this accuracy.

The convolution of a diffraction profile, by a gaussian function can be specified formally by (see Klug and Alexander, 1954, p. 246)

$$I_{2\theta} = \sum_{-\epsilon}^{+\epsilon} I'_{(2\theta+\epsilon)} \cdot e^{-k^2\epsilon^2} \cdot \Delta\epsilon,$$

where $I_{2\theta}$ is the convolved intensity at some specific 2θ, ϵ is a variable of the same units as 2θ, $I'_{(2\theta+\epsilon)}$ is the unconvolved intensity at $2\theta+\epsilon$, and k is the breadth constant.

PROFILES CALCULATED TO FIT SPECIFIC NATURAL ILLITE–MONTMORILLONITES

Materials

X-ray diffraction patterns were prepared from five representative mixed-layer illite–montmorillonite clays. These clays, and the X-ray methods used have been described by Hower and Mowatt (1966).

Procedure

Calculations of X-ray diffraction patterns shown on Figs. 1 and 2 are based on an invariant silicate skeleton (except for iron and potassium content)
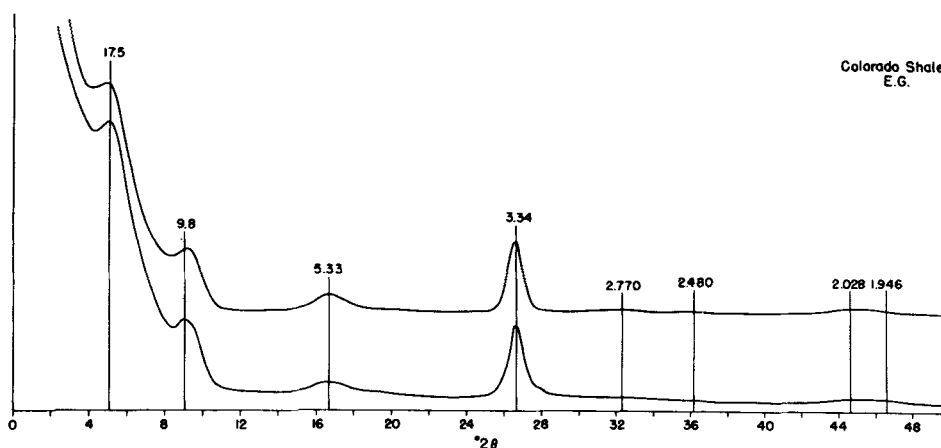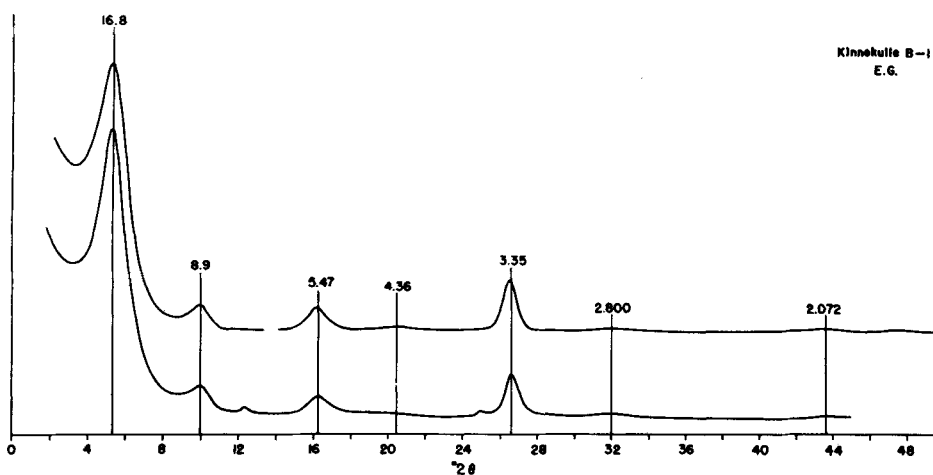

Fig. 1(c).

Fig. 1(d).

Fig. 1. Comparison of calculated diffraction profiles with X-ray patterns of ethylene glycol treated illite–montmorillonites. Top curves are calculated profiles, lower curves diffraction patterns.
(a) Kinnekulle A-2, 32% mont. layers, maximum *IM* ordering; (b) Two Medicine fm., 35% mont. layers, maximum *IM* ordering; (c) Colorado sh., 35% mont. layers, random with slight tendency to layer segregation ($P_{M.M} = 0.40$); (d) Kinnekulle B-1, 60% mont. layers, random.
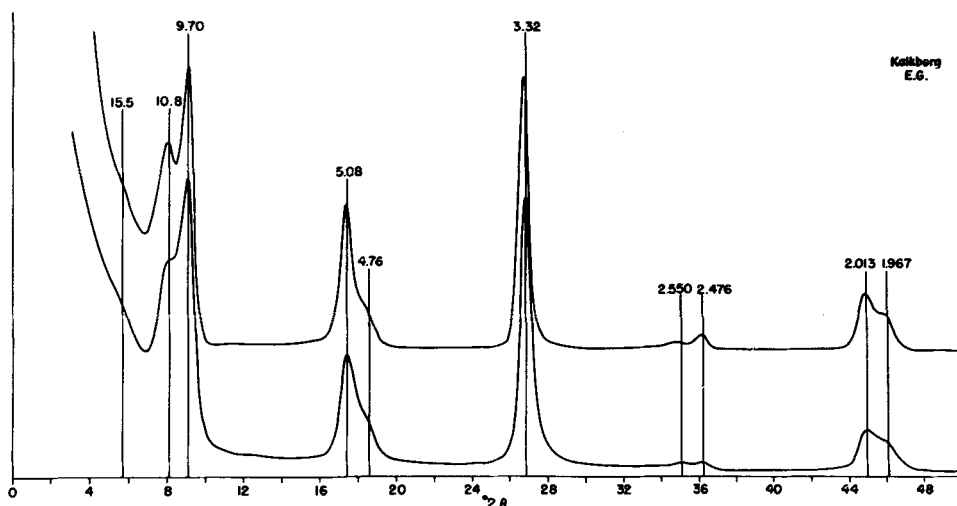
Fig. 2. Comparison of ethylene glycol threated Kalkberg bentonite with 10% mont. layer *IMII* superlattice calculated profile. Top curve calculated, lower curve diffraction pattern.

and glycol layer. Parameters for these units are given by Reynolds (1965), and are reiterated in Table 1. Iron and potassium contents were taken from analytical data (Hower and Mowatt, 1966). $d(001)$ values for illite and montmorillonite(glycol) were assumed, respectively, to be $10 \cdot 0$ Å and $16 \cdot 9$ Å. The approximate structure of ethylene glycol monoethyl ether (EGEE) adsorbed on montmorillonite $(d(001) = 15 \cdot 98$ Å) is reported by Reynolds (1969). All calculated profiles were diminished in intensity below $7 \cdot 8°$ 2θ by a function that simulated the effects of a one-degree beam slit in conjunction with a sample length of 4 cm. The random powder Lorentz-polarization factor was applied to all calculated profiles.

Variables optimized by trial and error methods

include (1) the proportion of expandable layers, (2) the ordering of expandable with respect to non-expandable layers, (3) the particle thickness distribution, and (4) the breadth constant for a gaussian convolution function.

When good agreement had been obtained between observed and calculated intensities for the various samples of montmorillonite(glycol)–illite, the optimized variables were retained, (except for the breadth constant) and the simulated diffraction patterns were recalculated with the substitution of EGEE in place of glycol. Samples of the clays were then centrifuged onto Al plates, solvated with EGEE, and analyzed by X-ray diffraction methods for comparison with calculated montmorillonite (EGEE)–illite profiles.

Table 1. Structural units assumed for illite and glycol–montmorillonite

	Atom type	Number of atoms	Atomic coordinates (Å)	Temperature factor B (Å^2)
Silicate skeleton	O	6	$3 \cdot 28$	1
	Si	4	$2 \cdot 68$	1
	O	6	$1 \cdot 07$	1
	Al, Fe	Specifiable Al + Fe = 2	0	1
Illite interlamellar space	K	Specifiable	0	1
Glycol interlamellar space	CH$_2$OH	$1 \cdot 7$	$2 \cdot 33$	11
	CH$_2$OH	$1 \cdot 7$	$1 \cdot 38$	11
	H$_2$O	$1 \cdot 2$	$0 \cdot 51$	11

RESULTS

Calculated and observed diffraction patterns are shown on Figs. 1 and 2 for the Kalkberg, Kinnekulle *B*, and Kinnekulle *A*-2 bentonites, and for the Two-Medicine and Colorado shales. On each figure, the upper trace represents the calculated profile. Vertical lines on each figure indicate the positions of the diffraction maxima on the observed traces. These lines were added so that the reader can observe any discrepancies between the observed and calculated spacings. Each line is labelled with a *d* value. Maxima on observed profiles that are not present on calculated profiles represent small amounts of other minerals present in the samples (e.g., a small amount of kaolin is present in Kinnekulle *B*-1, giving rise to small peaks at 12·3 and 24·8 degrees 2θ).

Table 2 lists the parameters of each of these structures that were optimized by trial and error methods. Figure 3 shows observed and calculated patterns for the Kalkberg, Kinnekulle *B*, and Kinnekulle *A* bentonites in which ethylene glycol monoethyl ether occupies the interlamellar positions in the expandable portions of the lattice.

DISCUSSION OF PATTERNS

Agreement between observed and calculated diffraction patterns is, for the glycol system, as close as could be expected between two specimen preparations from the same sample. The parameters which describe each of the structures (Table 2) are therefore as reliable as can be derived from diffraction patterns of the quality of those shown. The agreement between observed

Table 2. Parameters used to optimize illite–montmorillonite structures

| Sample	Fraction expandable	Type of ordering	Atoms Fe/2 octa positions	Atoms K/Illite unit	N and fraction N	Breadth constant (Glycol)	Breadth constant (EGEE)
Kinnekulle $B-1 < 1\mu$	60	Random	0·17	0·7	11(1)	2·45	2·0
Colorado shale $<0·5\mu$	35	Slight tendency toward segregation of mont.. $P_{M.M} = 0·40$	0·45	0·7	11(1)	2·30	
Kinnekulle *A*-2	32	Ordered; *IM* superlattice	0·1	0·7	3(0·05) 5(0·11) 7(0·17) 9(0·22) 11(0·28) 13(0·17)	2·70	1·5
Two-medicine	35	Ordered; *IM* superlattice	0·37	0·7	7–19, equal fractions	2·0	
Kalkberg	10	Ordered; *IMII* superlattice	0	0·8	3–19, equal fractions	3·5	2·5
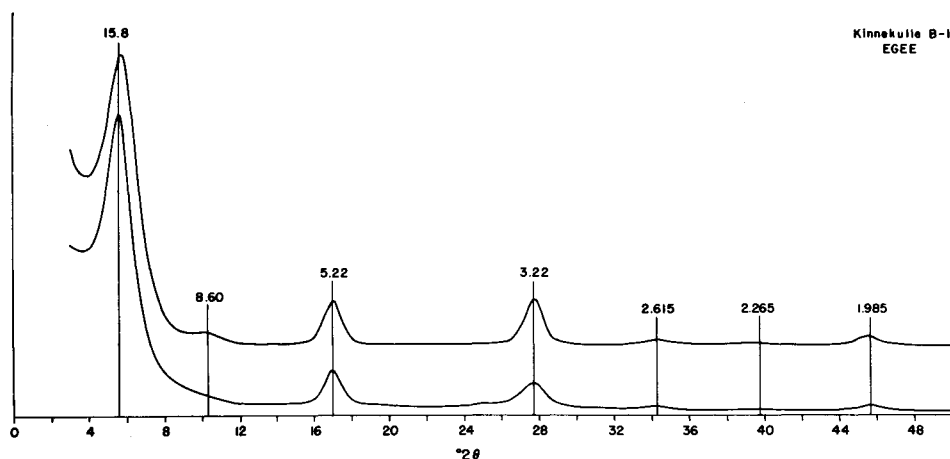
Fig. 3(a).
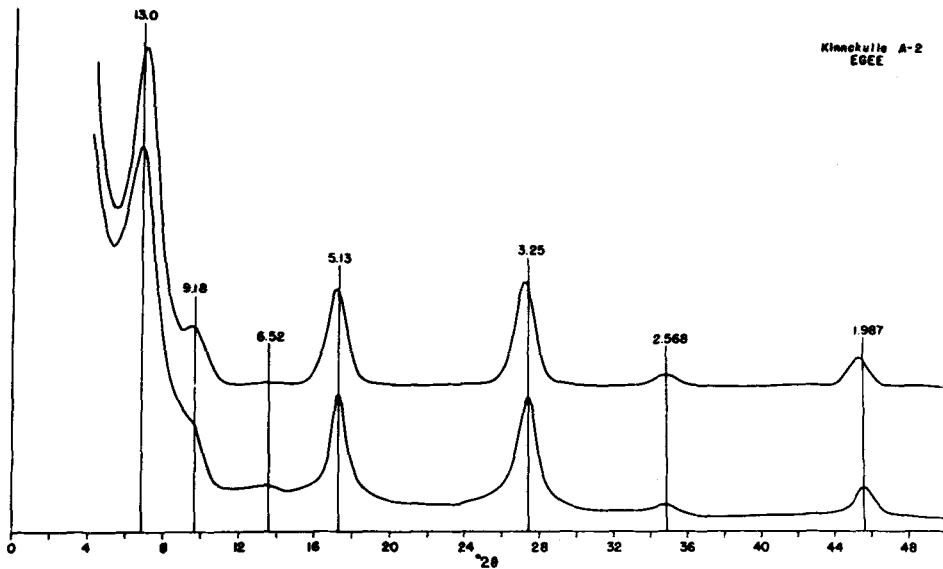
Fig. 3(b).
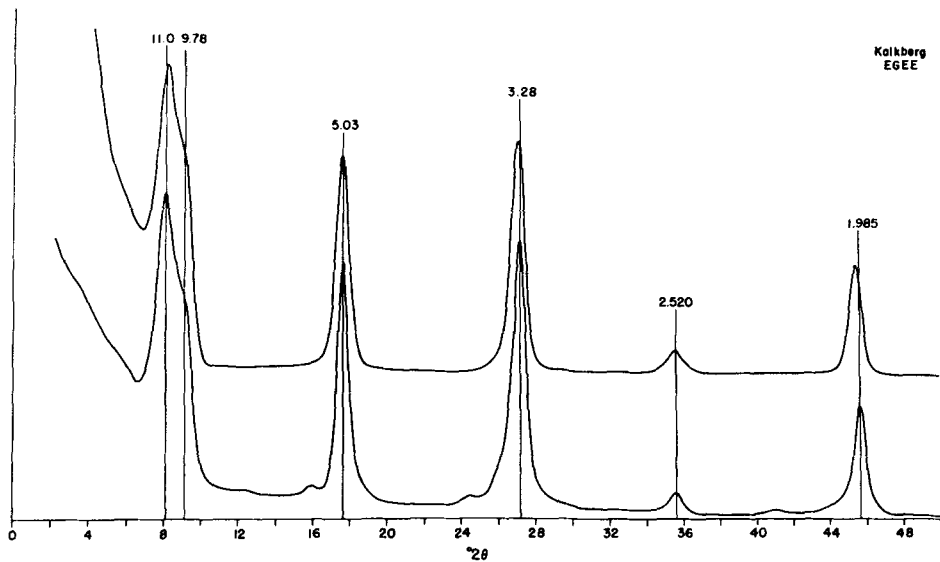
Fig. 3(c).

Fig. 3. Comparison of calculated diffraction profiles with X-ray patterns of ethylene glycol monoethyl ether treated illite–montmorillonites. Top curves are calculated, lower curves diffraction patterns. Assumed interstratification as in Figs. 1 and 2.
(a) Kinnekulle A-2; (b) Kinnekulle B-1; (c) Kalkberg bentonite.

and calculated results for EGEE-solvated clays (Fig. 3) is good, although discrepancies are greater than those observed for glycol-solvated clays (Figs. 1 and 2). Discrepancies of the order of $0.2°\,2\theta$ are evident in calculated maxima at high angles, and calculated intensity in the vicinity of $9°\,2\theta$ is higher than observed. The clays solvated with EGEE show broader maxima than the ones treated with glycol. The broadening does not seem to be markedly angle dependent, hence a distribution of slightly variable interlamellar (EGEE) spacings must be ruled out (analogous to strain

broadening in metals). Instrumental broadening should be similar for the glycol and EGEE solvated clay patterns, and therefore is probably not responsible for the differences. A smaller coherent scattering domain size could account for this increased broadening. Perhaps some interlamellar areas either do not expand with EGEE, or form structures that are disordered and random at small intervals. These comments are only speculations, and more work should be done on this problem. All of the discrepancies described above are minor, however, and in general, the EGEE system confirms the essential validity of the parameters of Table 2.

COMMENTS ON COMPUTER SIMULATED PROFILES

As a consequence of the examination of the patterns shown here, as well as hundreds of other calculated profiles prepared by the writers, some of which are shown in the Appendix, several observations should be made concerning the character of diffraction effects from interstratified montmorillonite(glycol)–illite. These are noted below.

(1) Peak migration

The analytical system of Mering (1949) suggests that, for random interstratification, mixed-layer maxima will appear intermediate to positions that would produce strong maxima from each of the primary phases involved in the interstratification. This principle is correct generally, but it is dangerous to apply indiscriminately. If the two primary maxima are widely separated, as for example the montmorillonite(glycol) 001 (16·9 Å) and the illite 001 (10·0 Å), then the 001/001 at 16·9 Å is merely deminished in intensity as the proportion of illite is increased. Little or no migration occurs (see Reynolds, 1967). On the other hand, calculations for interstratified Mg-vermiculite-mica show an 001/001 migration that accompanies compositional changes because the separation between the two primary maxima (14·3 Å and 10 Å) is significantly less. In patterns of montmorillonite(glycol)–illite, therefore, a peak between 10·0 and 16·9 Å indicates the presence of ordering, for this maximum contains as a dominant component, a higher order reflection from a superlattice.

Whether or not intermediate d-values are obtained from 001/001 or other maxima depends on the magnitudes and phases of the Fourier transforms of the layers (or superlattices) involved, the d-values for primary maxima, and the proportion of primary phases. The diffraction maxima are related to these factors in a sufficiently complex fashion so as to preclude an intuitive evaluation of expected diffraction effects. The predicted diffraction phenomena must be computed.

(2) Particle size effects

It has been shown (Reynolds, 1968; Ross, 1968) that diffraction maxima may be displaced from their normal positions by the effects of very fine particle size. Given the general form of the Fourier transform for most clays, these effects will be manifested most strongly in the region between $2\theta \approx 10°$ and $2\theta \approx 7°$. Hence it is recommended that when estimates of composition (proportion of primary types) are to be made from peak position, higher angle maxima be used. For the system montmorillonite-(glycol)-illite, the maximum between 16 and 18° 2θ is most suitable, for it shows conventionally accepted migration characteristics and is only slightly affected by particle size effects.

(3) Ordering

The ordering of primary layers to produce superlattice arrays profoundly alters the diffraction pattern, particularly at low angles, from the condition expected for random interstratification. As shown earlier in this work, ordering is common in montmorillonite–illite clays, and may involve non-nearest-neighbor effects (e.g., the Kalkberg). It is, in general, not possible to evaluate composition accurately from diffraction patterns of ordered materials until the type of ordering has been deduced. By a happy coincidence, however, the spacing of the maximum between 16 and 18° 2θ is almost identical, for a given composition, for cases of random interstratification and allevardite-like ordering. Hence it may be used to determine composition for the two most common types of interstratification found in the montmorillonite(glycol)–illite system. The maximum in the vicinity of 9° 2θ also gives similar results, but it is far more sensitive to particle-size effects.

Needless to say, these observations are difficult to apply to diffraction patterns from mixtures of clay minerals. For such samples, a final judgment concerning the types of separate phases, and the nature of any interstratification must be based on a consideration of the entire diffraction pattern, preferably one that extends to 50° 2θ. For complex samples that produce useful maxima only at low diffraction angle, as for example many soil clays, even a qualitative estimate of composition may be impossible by X-ray methods alone.

APPENDIX

The calculated profiles shown in the Appendix demonstrate the effects of ordering and com-

position on diffraction profiles in the system montmorillonite(glycol)–illite. Patterns representing random or nearest-neighbor ordering were computed according to the system described earlier (Reynolds, 1967) and amended in this paper. For these, the structural units shown in Table 1 were used, and Fe was taken as 0·15 and K as 0·7, except for the 0 and 10 per cent expandable cases, in which K is 0·95 and the atomic coordinate for oxygen (surface of silicate skeleton) is increased to 3·30 Å. All represent summations of 7, 8, 9, 10, 11, 12, and 13 silicate layers per crystallite, in equal proportions, and all were convolved with a gaussian function in which $k = 3·5$.

The three profiles for the $IMII$ superlattice case were computed according to the superlattice modification described above, and utilize the parameters of Table 1. For these, N is a summation between 3 and 19 in equal proportions, K is 0·8 and Fe = 0; these were also broadened by a guassian function in which $k = 3·5$.

These calculated profiles are meant to be of general use in the interpretation of diffraction patterns of mixed-layer illite–montmorillonites. The range of expandability presented for each type of interstratification is greater than the range known to the writers for natural materials. This greater range has been included so that the diffraction patterns of ordered and randomly interstratified illite–montmorillonites of the same composition can be compared. The sequences shown are: (1) random interstratification for 0, 10, 20, 40, 60, 80 and 100 per cent 16·9 Å layers (Fig. 4), (2) IM ordered (allevardite) interstratification for 10, 20, 30, 40, 60, and 80 per cent 16·9 Å layers (Fig. 5) (3) "half ordered" IM (i.e., $P_{II} = 0·5 P_I$) interstratification for 20, 40, 60, and 80 per cent 16·9 Å layers (Fig. 6), and (4) $IMII$ ordered interstratification for 5, 10, and 15 per cent 16·9 Å layers (Fig. 7). Table 3 presents data that can be used to construct migration curves for some of the more useful reflections. It must again be emphasized that although peak positions are necessary to the interpretation of diffraction patterns of illite–montmorillonites, the positions themselves are not generally sufficient. The peak positions depend on particle size distribution and ordering as well as the proportions of the layers involved. The data in Table 3 are therefore strictly valid only for the particle size distribution and degrees of ordering assumed in calculating the patterns. In addition, the reflections are often interfered with by other minerals present in the sample (particularly discrete illite) and peak positions must be determined with care.

Figures 8 and 9 are diffraction patterns of illite–montmorillonites covering the range of commonly occurring natural materials known to the writers. We have exlcuded the $IMII$ superlattice type (cf. Fig. 2). Additional data concerning these samples is presented in Table 4. Except for the unique allevardite, virtually all illite–montmorillonites with more than about 35–40 per cent montmorillonite layers are randomly interstratified. Samples A to D (with 100, 70, 50, and 40% montmorillonite layers) are of this type. We have observed a few samples of highly expandable illite–montmorillonites from bentonites that appear to be mixtures of randomly interstratified and IM ordered structures, but the results are not sufficiently clear to include.

The diffraction pattern of sample D is a good example of the danger of using peak positions only to determine the proportions of layers. It contains enough discrete illite so that the $(001)_{10}/(002)_{17}$ is not resolved, merging with the 10 Å peak. The $(002)_{10}/(003)_{17}$ is also seriously interfered with by the discrete illite (002). If one assumed the $(002)_{10}/(003)_{17}$ peak was single and determined its position by averaging, the result would be strongly biased toward too few montmorillonite layers. However, the low angle diffraction characteristics are distinctively those of a randomly interstratified illite–

Table 3. Peak positions (CuKₐ) and d-values for some reflections of illite-(glycol)montmorillonite

| Per cent expand-able	Refl.	Randomly interstratified				IM ordered				$(002)_{27}/(001)_{17or10}$			
		$(001)_{10}/(002)_{17}$		$(002)_{10}/(003)_{17}$		$(001)_{10}/(003)_{27}$		$(005)_{27}/(003)_{17}$		Max. ordering		0·5 ordered	
		2θ	d(Å)	2θ	d(Å)	2θ	d(Å)	2θ	d(Å)	2θ	d(Å)	2θ	d(Å)
0		8·68	10·18	17·65	5·02	8·68	10·18	17·65	5·02				
10		8·80	10·04	17·50	5·06	8·83	10·00	17·43	5·08				
20		8·92	9·91	17·19	5·15	9·09	9·72	17·03	5·20	6·83	12·93		
30						9·36	9·44	16·79	5·29	6·75	13·08	6·55	13·52
40		9·43	9·37	16·58	5·34	9·59	9·22	16·60	5·34	6·62	13·34	6·40	13·80
60		9·91	8·92	16·15	5·48	9·87	8·95	16·25	5·45	6·21	14·22	5·90	14·97
80		10·17	8·69	15·87	5·58	10·15	8·71	15·95	5·55	5·40	16·35	5·28	16·72
100		10·40	8·50	15·78	5·61	10·40	8·50	15·78	5·61	5·21	16·91	5·21	16·91
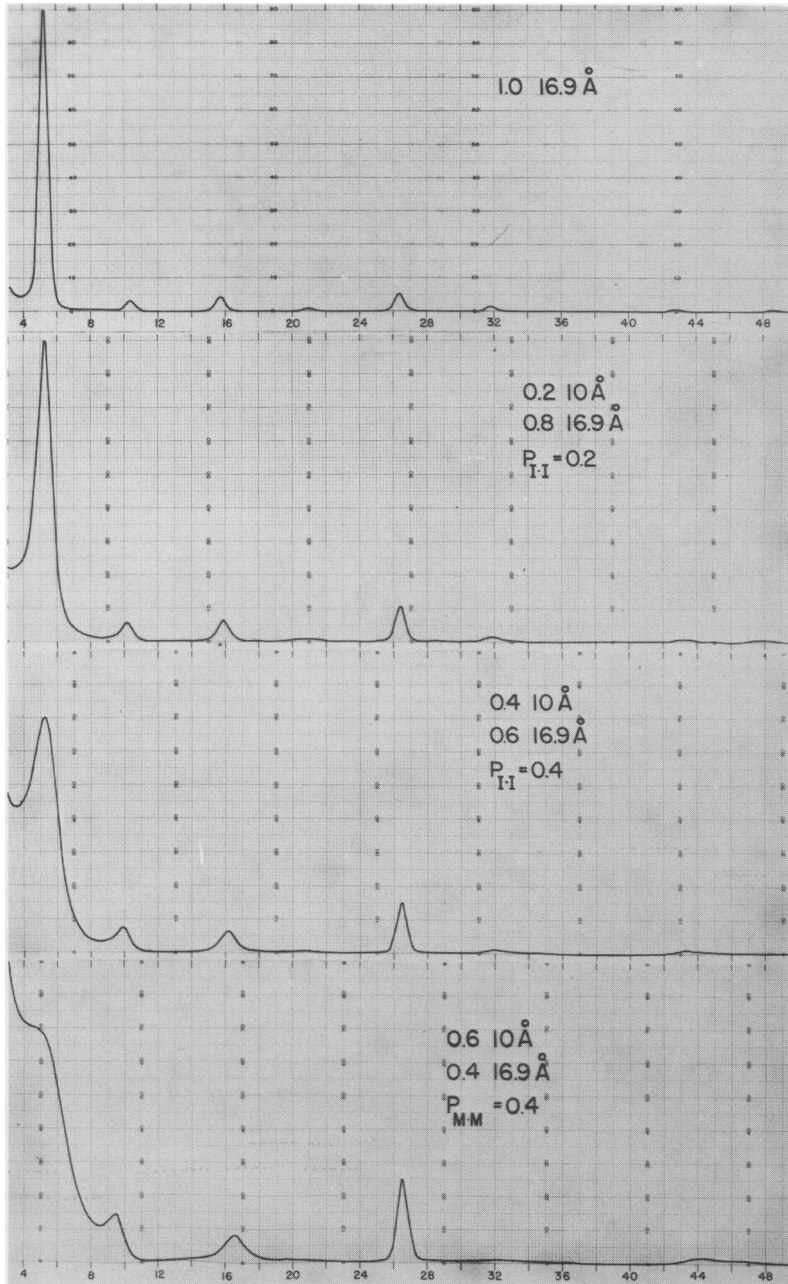
Fig. 4(a). Calculated diffraction profiles assuming random interstratification of 10 and 16·9 Å layers. Fraction of montmorillonite layers are 1·0, 0·8, 0·6 and 0·4.
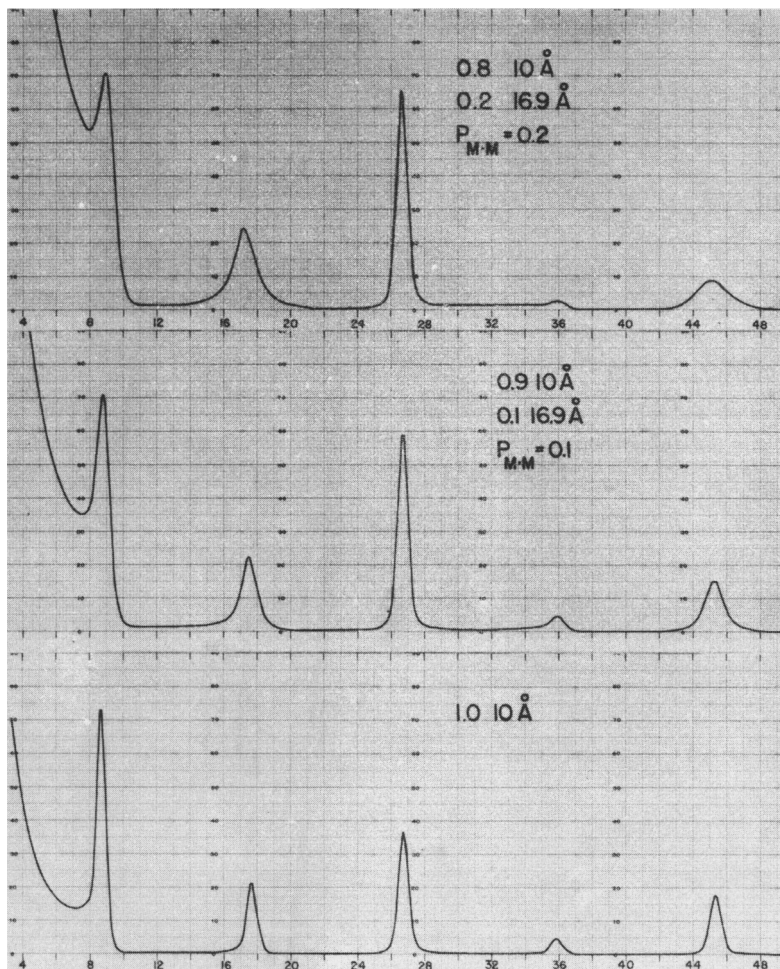
Fig. 4(b). Calculated diffraction profiles assuming random interstratification of 10 and 16·9 Å layers. Fractions of montmorillonite layers are 0·2, 0·1 and 0.
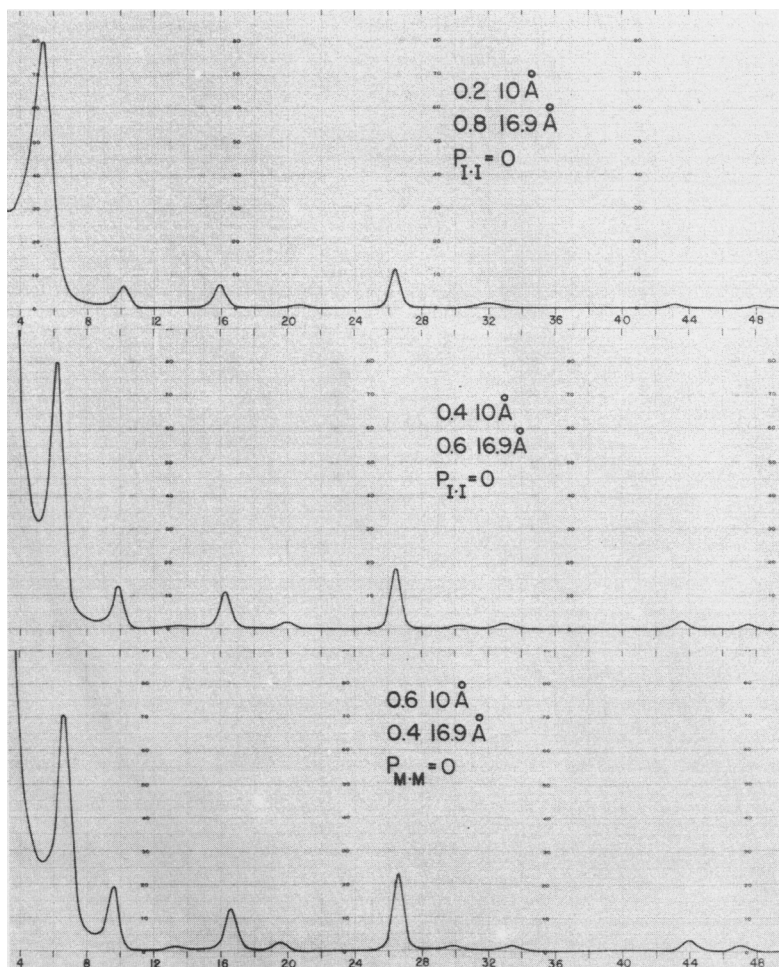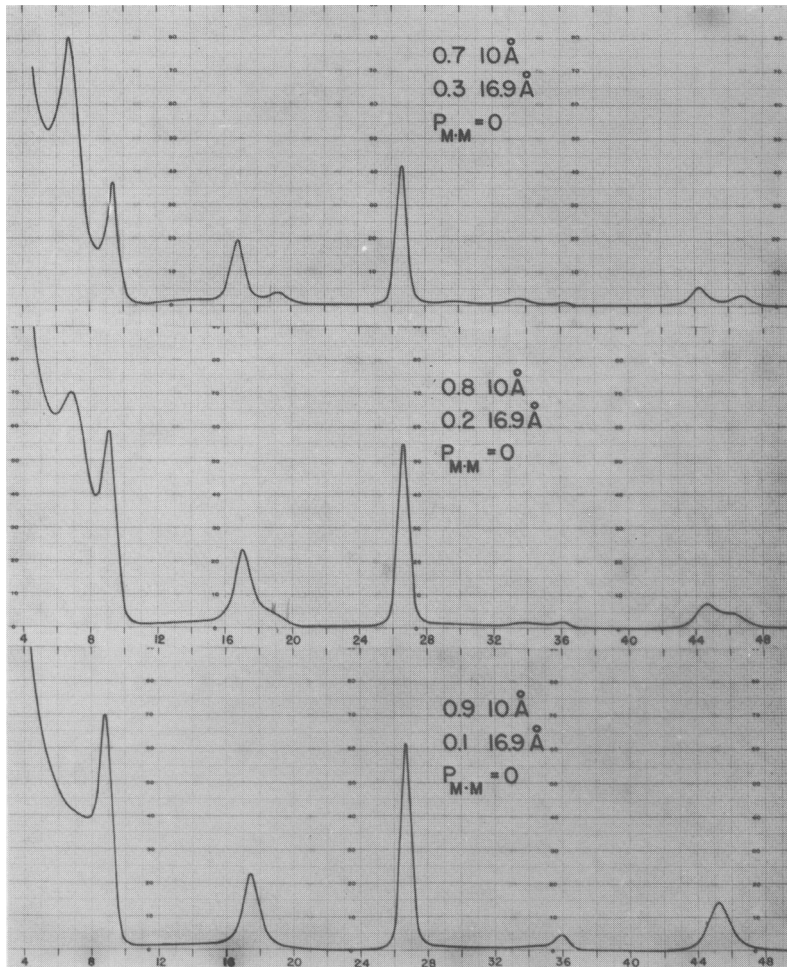
Fig. 5(a). Calculated diffraction profiles assuming maximum allevardite-like (*IM*) ordered interstratification possible of 10 and 16·9 Å layers. Fractions of montmorillonite layers are 0·8, 0·6 and 0·4.

Fig. 5(b). Calculated diffraction profiles assuming maximum allevardite-like (*IM*) ordered interstratification possible of 10 and 16·9 Å layers. Fractions of mont-morillonite layers are 0·3, 0·2 and 0·1.

Fig. 6. Calculated diffraction profiles assuming 0·5 maximum allevardite-like (*IM*) ordered interstratification possible of 10 and 16·9 Å layers. Fractions of mont-morillonite layers are 0·8, 0·6, 0·4 and 0·2. For comparison with random and maximum ordered profiles.
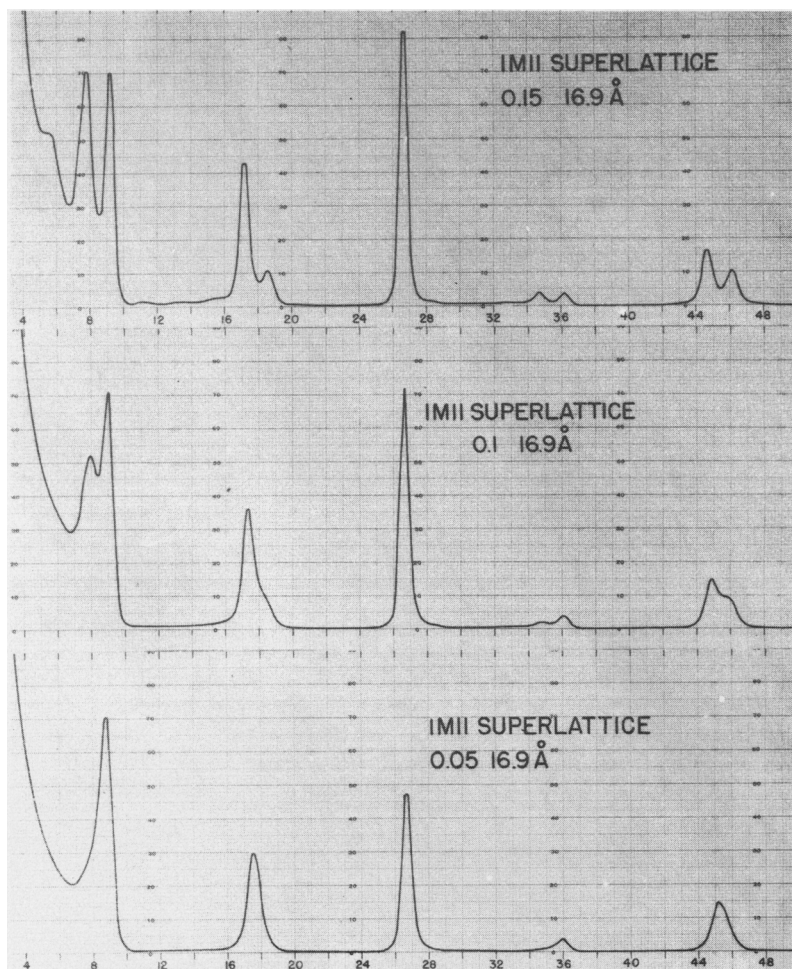
Fig. 7. Calculated diffraction profiles assuming random interstratification of *IMII* superlattice units with *I* layers. Fractions of montmorillonite layers are 0·15, 0·10 and 0·05.
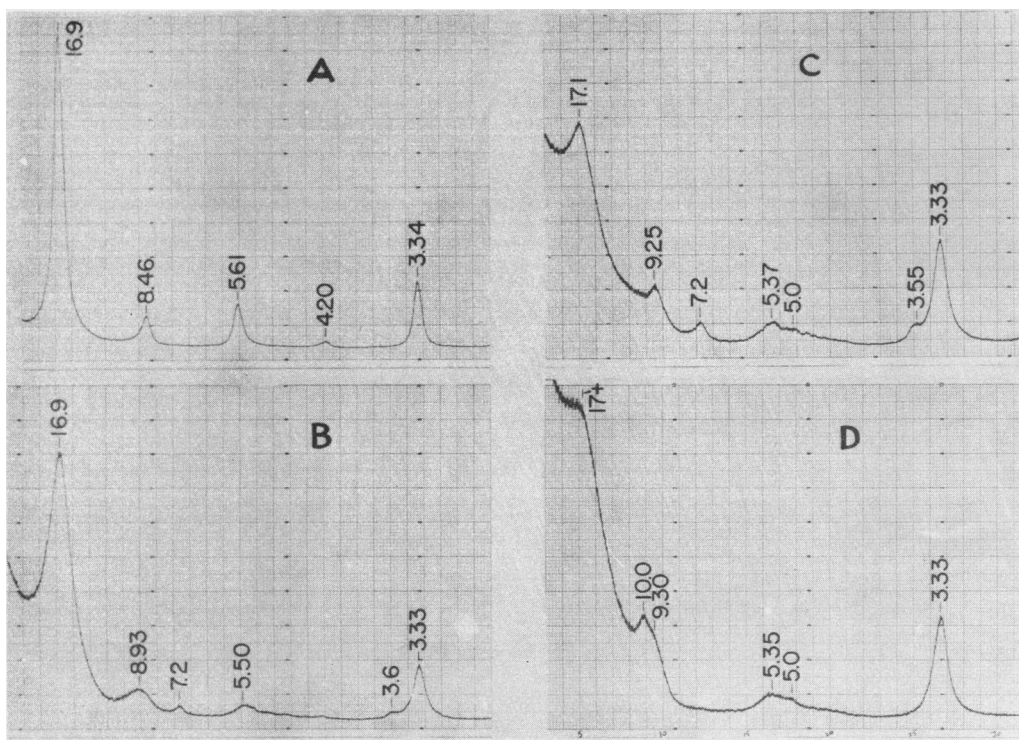
Fig. 8. Diffraction patterns of ethylene glycol treated samples of montmorillonite, and randomly interstratified illite–montmorillonites. Percentages of montmorillonite layers: *A.* 100, *B.* 70, *C.* 50, and *D.* 40. See Table 3 for additional information.
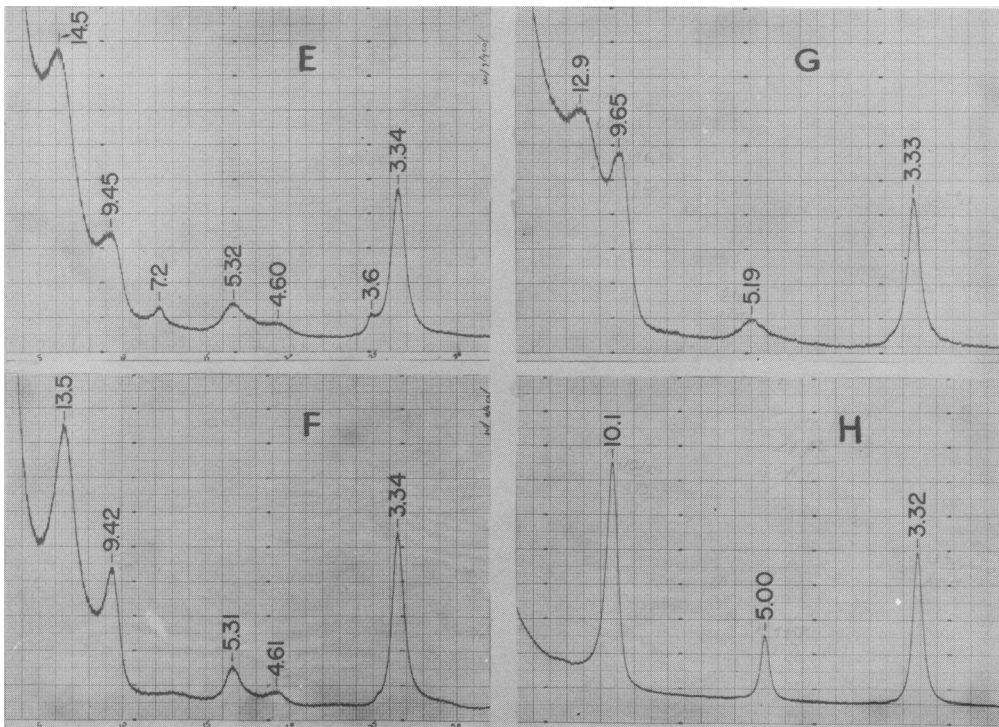
Fig. 9. Diffraction patterns of ethylene glycol treated samples of illite and *IM*-ordered illite–montmorillonites. Percentages of montmorillonite layers: *E*. 35, <0·5 *IM* ordered, *F*. 30, *G*. 20, *H*. 0 (illite).

Table 4. Additional data for samples whose diffraction patterns are shown in Figs. 8 and 9

	Occurrence	Illite–mont. type	Other Minerals
A	Bentonite, Colorado sh., Great Falls, Montana	100% mont.	none
B	Mudstone, Two Medicine fm., Cut Bank, Montana	65–70% mont. randomly interstratified	small amount of kaolin
C	Shale from Dakota SS., Golden, Colorado	50% mont., randomly interstratified	some kaolin, small amount of discrete illite
D	Sundance fm., Thermopolis. Wyoming	40% mont., randomly interstratified	some discrete illite
E	Mudstone, Two Medicine fm., Choteau, Montana	35–40% mont., probably <0·5 *IM* ordered	some kaolin
F	Mudstone, Two Medicine fm., Bowman's Corner, Montana	35% mont., *IM* ordered	none
G	Mudstone, Two Medicine fm., Wolf Creek, Montana	20% mont., *IM* ordered	none
H	Silver Hill fm., Jefferson Canyon, Montana	0% mont.	none

montmorillonite with 40 per cent expanded layers.

Virtually all illite–montmorillonites with expandabilities ≤35 per cent are either *IM* or *IMII* ordered, with the latter type restricted to 5–10 per cent montmorillonite layers. Examples of *IM* ordered minerals are shown in Fig. 9 (patterns *E* to *H* with 35–40, 35, 20, and 0 per cent montmorillonite layers) are of this type. Only sample *E*, with the highest expandability seems to have less than the maximum possible *IM* ordering.

CONCLUSIONS

X-ray diffraction patterns of oriented specimens of illite–montmorillonites can be precisely duplicated by calculated one-dimensional diffraction profiles in which the variables particle size, chemical composition, convolution factors, proportions of layers, and manner of interlayering are treated. The results indicate that illite–montmorillonites with expandabilities of above 35–40 per cent are almost always randomly interstratified and those of lower expandabilities have ordered interstratification of either the allevardite (*IM* superlattice) or *IMII* type. Allevardite-like ordering predominates, with the *IMII* superlattice type confined to samples with 5–10 per cent montmorillonite layers.

Quite accurate interpretation of the proportions of layers and interlayering type in illite–montmorillonites is possible when using both peak position and comparison of the low angle diffraction characteristics with calculated profiles.

REFERENCES

Brindley, G. W. (1956) Allevardite, a swelling double-layer mica mineral: *Am. Mineralogist* **41**, 91–103.

Burst, J. F. (1969) Diagenesis of Gulf Coast clayey sediments and its possible relation to petroleum migration: *Bull. Am. Assoc. Petrol. Geol.* **53**, 73–93.

Bystrøm, A. M. (1954) Mineralogy of the Ordovician bentonite beds at Kinnekulle, Sweden: *Sveriges Geol. Undersökn. Arsbok* **48**, No. 5, 62 pp.

Hamilton, J. D. (1968) Trimorphic clay minerals from the Lower Hunter Permian succession of New South Wales: *J. Geol. Soc. Australia* **15**, 9–24.

Hendricks, S. B. and Teller E. (1942) X-ray interference in partially ordered lattices: *J. Chem. Phys.* **10**, 147–167.

Hower, J. and Mowatt T. C. (1966) The mineralogy of illites and mixed-layer illite–montmorillonites: *Am. Mineralogist* **51**, 825–854.

Klug, H. P. and Alexander L. E. (1954) *X-Ray Diffraction Procedures*, Wiley, New York 716 pp.

Lippman, F. (1954) Über einen Keuperton von Zaiserweiher bei Maulbronn: *Heidelberger Beitr. Mineral. Petrog.*, Bd. 4, **5**, 130–134.

MacEwan, D. M. C. (1958) Fourier transform methods for studying scattering from lamellar systems: II, The calculation of X-ray diffraction effects for various types of interstratification: *Kolloid-Z.* **156**, 61–67.

MacEwan, D. M. C., Ruiz Amil, A. and Brown G. (1961) Interstratified clay minerals: in G. Brown, Ed., X-ray identification and crystal structures of clay minerals: *Mineral. Soc. London*, 393–445.

Maiklem, W. R. and Campbell F. A. (1965) A study of the clays from Upper Cretaceous bentonites and shales in Alberta: *Can. Mineralogist* **8**, 354–371.

Méring, J. (1949) L'interférence des rayon-X dans les systemes à stratification desordonée: *Acta Crystallogr* **3**, 371–377.

Perry, E. and Hower J. (1969) Burial diagenesis in Gulf Coast pelitic sediments: *18th Clay Min. Conf. (Abst)*.

Reynolds, R. C. (1965) An X-ray study of an ethylene glycol–montmorillonite complex: *Am. Mineralogist* 990–1001.

Reynolds, R. C. (1967) Interstratified clay systems: calculation of the total one-dimensional diffraction function: *Am. Mineralogist* **52**, 661–672.

Reynolds, R. C. (1968) The effect of particle size on

apparent lattice spacings: *Acta Crystallogr* **A24**, 319–320.

Reynolds, R. C. (1969) Orientation of ethylene glycol monethyl ether molecules on montmorillonite: *Am. Mineralogist* **54**, 562–567.

Ross, M. (1968) X-ray diffraction effects by non-ideal crystals of biotite, muscovite, montmorillonite, mixed-layer clays, graphite, and periclase: *Z. Krist.* **126**, 80–97.

Ruiz Amil, A., Ramírez García, A. and MacEwan D. M. C. (1967) X-ray diffraction curves for the analysis of interstratified structures: *Inst. de Quimica Inorg., Cons. Sup. Inres. Cientificas, Madrid.* Volturna Press.

Sato, M. (1965) Structure of interstratified (mixed-layer) minerals: *Nature* **208**, 70–71.

Velde, B. (1969) The compositional join muscovite-pyrophyllite at moderate pressures and temperatures; *Bull. Soc. Franc. Mineral. Crist.* **92**, 360–368.

Weaver, C. E. (1956) Distribution and identification of mixed-layer clays in sedimentary rocks: *Am. Mineralogist* **41**, 202–221.

Résumé – Des recherches ont été effectuées sur la nature de l'interstratification dans les illites-montmorillonites à feuillet interstratifiés, en les comparant aux modèles de diffraction du glycol éthylène et d'échantillons traités à l'éther monoéthyl de glycol éthylène avec des courbes de diffraction à une dimension. Les courbes calculées prennent en considération les effets de la distribution de grandeur de la particule, de la composition chimique et des facteurs de convolution de même que les rapports des feuillets et du type de stratification. Sur la base des comparaisons détaillées concernant les modèles de diffraction des illites-montmorillonites monominéraliques appartenant à une composition chimique connue, on en a conclu qu'il existe trois types d'interstratification; (1) au hasard, (2) un ordre de la forme allevardite (3) et des unités ayant un super réseau comprenant des couches de trois illites et un montmorillonite (IMII). Par suite de la comparaison des séries de courbes calculées avec les modèles de diffraction des nombreux échantillons d'illite-montmorillonites, on en a conclu que virtuellement tous les illites-montmorillonites ayant des dilatations de l'ordre de 40–100 pour cent environ, sont interstratifiés au hasard (l'allevardite étant l'exception): à moins de 40 pour cent, les feuillets de montmorillonites ont presque toujours une interstratification ordonée. L'ordre de la forme de l'allevardite est prédominant dans les illistes-montmorillonites qui ont une interstratification ordonnée, avec les variétés du super réseau IMII confinées à des échantillons ayant des feuillets de montmorillonite d'environ 10 pour cent.

Kurzreferat – Das Wesen der Zwischenlagerung in gemischtschichtigen Illit–Montmorilloniten wurde untersucht durch Vergleich von Beugungsmustern von mit Äthylenglykol und Äthylenglykol-monoäthyl Äther behandelten Proben mit berechneten, eindimensionalen Beugungsprofilen. Die berechneten Profile berücksichtigen die Wirkungen der Teilchengrössenverteilung, der chemischen Zusammensetzung und der Zusammenrollungsfaktoren sowie die Proportionen der Schichten und den Zwischenlagerungstyp. Auf Grund einer detaillierten Anpassung von Beugungsmustern mono-mineralischer Illit–Montmorillonite bekannter chemischer Zusammensetzung wird der Schluss gezogen, dass es drei Arten von Zwischenlagerung gibt, nämlich (1) zufallsmässige, (2) allevardit-artige Ordnung und (3) Supragittereinheiten aus drei Illit und einem Montmorillonit bestehend (IMII). Durch Vergleich von Folgen berechneter Profile mit den Beugungsmustern verschiedener Proben von Illit–Montморilliniten wird festgestellt, dass beinahe alle Illit–Montmorillonite mit Ausdehnungsvermögen von etwa 40 bis 100 Prozent aufallsmässige Zwischenlagerung aufweisen (ausnahmsweise auch Allevardit); bei < 40 Prozent Montmorillonitschichten besteht fast immer geordnete Zwischenlagerung. In den Illit–Montmorilloniten mit geordneter Zwischenlagerung herrscht die allevarditartige Odnung vor, während die IMII Supragitter Arten auf Proben mit etwa 10 Prozent Montmorillonitschichten beschränkt bleiben.

Резюме — Характер чередования слоев в смешанно-слойных иллит-монтмориллонитах был исследован в результате сравнения дифракционных картин образцов, насыщенных этилен-гликолем и этилен-гликоль-моноэтилэфиром, с вычисленными одномерными дифракционными профилями. При вычислении профилей были приняты во внимание эффекты распределения размеров частиц, химического состава, факторов свертки, а также относительные количества и тип чередования слоев. В результате тщательного подбора согласующихся с теоретическими кривыми дифракционных картин мономинеральных иллит-монтмориллонитов с известным химическим составом, сделан вывод о наличии трех типов чередования слоев: 1) беспорядочного, 2) алевардитового упорядочения и 3) с образованием сверхструктурных элементов, состоящих из трех иллитовых и одного монтмориллонитового слоев (ИМИИ). При сопоставлении вычисленных профилей интенсивности с дифракционными картинами многих образцов иллит-монтмориллонитов установлено, что фактически все иллит-монтмориллониты с разбухаемостью примерно от 40 до 100% являются беспорядочно смешанно- слойными (за исключением алевардита), при менее 40% монтмориллонитовых слоев почти всегда имеет место упорядоченное чередование слоев. Алевардитовое упорядочение преобладает в иллит-монтмориллонитах с упорядоченным чередованием слоев, тогда как сверхструктурные разновидности ИМИИ возможны лишь в образцах, содержащих приблизительно 10% монтмориллонитовых слоев.